Real-Time Method for Motion-Compensated MR Thermometry and MRgHIFU Treatment in Abdominal Organs

Zarko Celicanin,[1,2]* Vincent Auboiroux,[3] Oliver Bieri,[1] Lorena Petrusca,[3] Francesco Santini,[1] Magalie Viallon,[3] Klaus Scheffler,[2,4] Rares Salomir[3]

Purpose: Magnetic resonance-guided high-intensity focused ultrasound is considered to be a promising treatment for localized cancer in abdominal organs such as liver, pancreas, or kidney. Abdominal motion, anatomical arrangement, and required sustained sonication are the main challenges.

Methods: MR acquisition consisted of thermometry performed with segmented gradient-recalled echo echo-planar imaging, and a segment-based one-dimensional MR navigator parallel to the main axis of motion to track the organ motion. This tracking information was used in real-time for: (i) prospective motion correction of MR thermometry and (ii) HIFU focal point position lock-on target. Ex vivo experiments were performed on a sheep liver and a turkey pectoral muscle using a motion demonstrator, while in vivo experiments were conducted on two sheep liver.

Results: Prospective motion correction of MR thermometry yielded good signal-to-noise ratio (range, 25 to 35) and low geometric distortion due to the use of segmented EPI. HIFU focal point lock-on target yielded isotropic in-plane thermal build-up. The feasibility of in vivo intercostal liver treatment was demonstrated in sheep.

Conclusion: The presented method demonstrated in moving phantoms and breathing sheep accurate motion-compensated MR thermometry and precise HIFU focal point lock-on target using only real-time pencil-beam navigator tracking information, making it applicable without any pre-treatment data acquisition or organ motion modeling. **Magn Reson Med 72:1087–1095, 2014. © 2013 Wiley Periodicals, Inc.**

Key words: MRgHIFU; mobile organ; temperature mapping; motion correction; dynamic HIFU-beam steering

INTRODUCTION

Magnetic resonance-guided high-intensity focused ultrasound (MRgHIFU) is considered a promising approach for noninvasive and spatio-temporal controlled tissue ablation (1,2). Its applicability to the clinical field has been demonstrated primarily in the treatment of uterine fibroids (3,4), breast cancer (5), and prostate cancer (6), while ultrasound-triggered local drug delivery was under investigation in vivo (7). Treatment of organs located in the upper abdomen could benefit from this technology, but significant improvement of the clinical treatment method is required. Respiratory and other physiological motion makes treatment difficult, because MR thermometry (MRT) is affected by organ motion, and it also requires continuous correction of the HIFU focal point position, while the rib cage reduces the available acoustic window hindering effectiveness of tissue ablation. Prevention of collateral heating and thermal coagulation of ribs and their surrounding tissue has to be considered in cases when upper abdominal organs are to be treated by HIFU. Rib sparing procedures have been reported in the past (8,9), while in Salomir et al (10) a dedicated MR-guided positioning method of specific reflective strips for acoustic masking of the ribs has been suggested. Although respiratory gated treatment approaches have been reported (11,12), sustained sonication is still preferred due to the high perfusion rates of organs such as liver and kidney, increased treatment duration for gated approach, and differing breath-hold positions of different gating windows.

The first report on irregular motion correction in MR-guided focused ultrasound thermotherapy (13) described the use of MR navigator echoes, in-plane registration of the images as post-processing, and redefinition of the reference phase map following the motion. The MRgHIFU treatment method, reported in de Senneville et al (14), was based on fast MR thermometry and advanced image post-processing to extract organ motion displacement in real-time. Modeling of organ motion was performed during a so-called initial learning phase, while during the treatment, the motion field of the most similar image was used retrospectively to correct the focal point position. This method required the hypothesis of a periodical motion, because the focal point position was extrapolated for the next cycle. The delay of estimation was around 2 s, and thus not negligible, which imposed restriction of high periodicity of the motion pattern, and was incapable of handling non-rigid deformations caused

[1]Department of Radiology, Division of Radiological Physics, University of Basel Hospital, Basel, Switzerland.

[2]MRC Department, MPI for Biological Cybernetics, Tübingen, Germany.

[3]Radiology Department, University of Geneva, Geneva, Switzerland.

[4]Department of Biomedical Magnetic Resonance, University of Tübingen, Tübingen, Germany.

Grant sponsor: National Foundation of Science, Switzerland; Grant number: CR32I3-125499 and CR33I3_143980.

*Correspondence to: Zarko Celicanin, Dipl.-Ing., Division of Radiological Physics, Department of Radiology, University of Basel Hospital, Petersgraben 4, 4031 Basel, Switzerland. E-mail: zarko.celicanin@unibas.ch

Received 21 June 2013; revised 27 September 2013; accepted 7 October 2013

DOI 10.1002/mrm.25017
Published online 14 November 2013 in Wiley Online Library (wileyonlinelibrary.com).

by intestinal activity or muscle relaxation. In (15), the previous work was improved by reducing the delay with predictive filtering, while the out-of-plane motion was compensated by an one-dimensional (1D) pencil-beam navigator. In de Senneville et al (16), an optimized principal component analysis (PCA)-based motion descriptor was used to characterize organ motion during treatment. During a so-called preparative learning step, the PCA was used to detect spatio-temporal coherences in the organ motion, which were later used during treatment for the adjustment of the beam position and the compensation of motion-related errors in thermal maps. In Holbrook et al (17), a recent method was reported for focus steering dedicated to periodic motion, using a retrospective lookup table of images correlated to the breathing signal by assuming a regular pattern of respiratory motion. Although the previous work represents significant progress toward safe and successful MRgHIFU treatment of abdominal organs, there are still important issues to be resolved. Neither of the previous solutions tried to use any prospective motion correction for improved MR thermometry accuracy, although it meant imaging with heavily T_2* weighting and low signal-to-noise ratio (SNR). Methods for temperature mapping and/or motion compensation requiring acquisition of baselines during the preparative learning step are incapable of dealing with aperiodic motion and are prone to significant inaccuracy after short time (5-10 min) due to the drifting organ motion (18). The necessity of periodically updating look up tables may yield workflow drawbacks.

Recently, hybrid ultrasound-MR guided HIFU sonication was reported in (19,20), using an optical flow tracking in ultrasound images to obtain organ motion information. Although accurate performance of the method was demonstrated, additional instrumentation complicates the set-up.

Motion artifacts can be classified in two categories based on the time scale of motion with respect to the image acquisition time. Physical displacement of the spins of an imaging object during the MR image acquisition causes an intrascan motion artifact, which manifests itself as blurring and ghosting, which can be surmounted by accelerating acquisition rate in a trade-off between acquisition time on one side, and SNR and temperature accuracy on the other. The interscan motion, the movement of organs during the period between the consecutive slice acquisition, does not affect image quality directly, but complicates the reconstruction of temperature map and thermal dose. Non-invasive temperature measurement based on temperature-sensitive MR proton resonance frequency (PRF) shift is currently the preferred method of choice due to its excellent linearity and near independence of tissue type (21).

Tissue motion is the most challenging problem of PRF shift-based MRT, and it hinders clinical applications of MRgHIFU that involve organ motion. A reference-less MRT method (22,23) uses the phase information from outside the heated region to estimate the background phase inside the region of interest, unlike the standard baseline MRT method which is based on subtraction of temporal reference phase maps acquired before heating. The reference-less method is preferable in terms of robustness against tissue motion and magnetic perturbations, permitting also interactive repositioning of MR thermometry slices if required. The benefits of reference-less and multi-baseline temporal referenced methods can be obtained with a combined approach (24).

Respiratory induced patterns of organ motion in the abdomen were quantitatively and qualitatively examined by varies groups (25,26). Liver motion driven by the diaphragm is predominantly along the superior-inferior (S/I, equivalent cranial–caudal) direction and its largest extent appertains to regions below the diaphragm. An intersubject modeling of liver deformation during quasi-periodic respiratory motion was reported in von Siebenthal et al (26). The principal component of liver motion is along SI direction, enabling a 1D navigator to track it.

Unlike the retrospective motion correction (27), the prospective motion correction (28) (PMC) is applied before the acquisition of a complete set of raw image data. The PMC can be implemented with MR navigator echoes (29) that are used for tracking organ motion during k-space acquisition, and based on this information subsequent correction of slice position and orientation in real-time is applied by adjusting MR pulse sequence acquisition parameters, ensuring steady acquisition in the anatomy of interest.

Here, a novel MRgHIFU treatment method is presented, where tracking of the organ motion, carried out by MR navigator echo originally suggested in (29) and further refined in Nehrke et al (30), provides real-time organ position information which is used for HIFU focal point position correction and PMC of MRT simultaneously. To the best of the authors' knowledge, this is the first attempt of using near real-time organ motion tracking for PMC of MR thermometry and simultaneous HIFU beam steering requiring neither preparative learning step nor any organ motion modeling, i.e., prediction of organ motion. The novel developments reported here, are parts of a long-term project, and the motion-compensation system was added on top of our previously described methodological functionalities.

METHODS

MR Thermometry

All experiments were performed on a 3 Tesla (T) whole-body MRI clinical scanner (MAGNETOM Trio - A TIM System, Siemens Medical Solutions, Erlangen, Germany).

Real-time PRF shift-based MR thermometry based on RF-spoiled lipid-suppressed, using 1-2-1 binomial frequency-selective RF pulse, segmented gradient-recalled echo (GRE) echo-planar imaging (EPI), was modified to acquire a 1D MR navigator echo (pencil-beam navigator) before each segment of k-space (pulse sequence principle, navigator profiles and a navigator histogram are shown on Fig. 1). Flow compensation was available in the sequence (nulling the first moment of the gradient). MRT slice position was readjusted, facilitating motion correction on a segment-per-segment basis using the real-time feedback prospective motion correction (PACE) method, available on the clinical Siemens scanner, based on the tissue displacement information measured by the MR navigator echo. Note that the

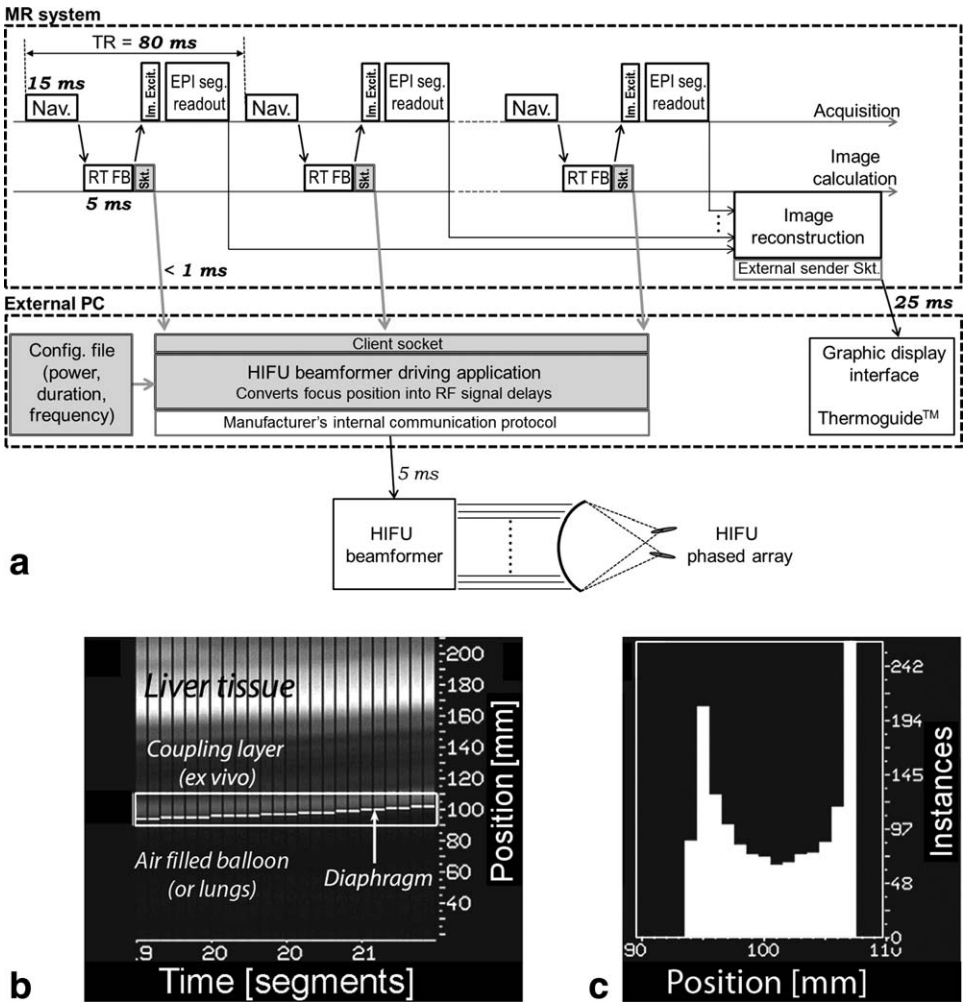

FIG. 1. **a:** Comprehensive system architecture diagram for the motion-compensated MRgHIFU treatment. Standard subsystems are shown as white background boxes, while custom built ones are represented with shaded background boxes. Time delays for data acquisition, calculation and transfer inside the system are indicated. Pulse sequence diagram of principle is shown inside the MR system providing details of real-time navigator feedback functionality, which communicates the tracking information for HIFU focal point position correction and PMC of MRT. (RT FB, real-time feedback; Skt., socket; Nav., navigator; Im. Excit., image excitation). **b:** Navigator profiles with real-time extraction of motion information. **c:** Histogram of the tracked feature positions along the direction of the navigator.

motion correction sampling time is equal to TR and thus much shorter than the temporal resolution of MR thermometry. This approach achieved the intrascan motion correction. For future compatibility with more complex correction of the motion, the 1D navigator feedback data was converted into full 3D spatial coordinates of the scanner reference system, knowing the orientation vector of that user-defined navigator (e.g., parallel to the Oz-axis of the scanner). For the current implementation, the vector's coordinates perpendicular to the SI direction were zero-filled when sent to the HIFU beamformer. These spatial coordinates were fed in real-time to a HIFU system to adapt focal point position accordingly, as shown on Figure 1a, which also provides detailed information on system architecture and latencies. The following acquisition parameters were used for MR thermometry: echo time/repetition time (TE/TR) = 8.69/80 ms, EPI factor = 9, slice thickness = 5 mm, in-plane resolution = 1.5 × 1.5 mm^2 ex vivo and 1.88 × 1.88 mm^2 in vivo, readout bandwidth 700 Hz/pixel, reconstructed image matrix = 128 × 128, acquisition time per slice = 1.04 s.

The pencil-beam navigator was used for slice tracking of MR thermometry. It comprised of a 2D spatially selective echo-planar RF pulse, used to excite a pencil-beam-shaped column, followed by a gradient echo. The acquisition duration of the pencil-beam navigator was approximately 20 ms, while the navigator volume was a rectangular column with dimensions of (5 to 10) × (5 to 10) × 180 mm. Note that the TR parameter provided above, also includes the duration of the navigator. Exemplary navigator profiles and a histogram of motion tracking ex vivo are shown on Figure 1b and 1c, respectively.

Magnitude and phase images were sent in real-time to an external computer and used for temperature visualization and control of the HIFU platform.

The temperature elevation profile was calculated on the external computer based on the reference-less method (for details, cf. Salomir et al) (23), which exploits mathematical properties of the magnetic field in a near-homogeneous medium and reconstructs the background phase inside the region of interest by solving a 2D Dirichlet problem based on iterative convolution. This calculation was performed with a typical ROI diameter of 20 to 25 pixels, requiring less than 50 ms of CPU time, making the temperature and thermal dose subsequently available in real-time. The calculation ROI was set larger in motion non-compensated sonications to encompass the elongated thermal build-up in the focal plane.

MR-Guided HIFU Platform

The randomized 256-element phased-array transducer (Imasonic, Besançon, France) was used for the MRgHIFU experiment with the following characteristics: frequency range = 974-1049 kHz, natural focal length = 130 mm, aperture = 140 mm, diameter of each element = 6.6 mm. The HIFU transducer was driven by a 256-channel beam former (Image Guided Therapy, Pessac-Bordeaux, France). Electronic steering of the focal point was performed within -3 dB revolution ellipsoid of axes 30 mm (Ox), 30 mm (Oz), and 50 mm (Oy) around the natural focus. The maximum switching rate of the beam-former's RF signals to change the focal point position was 20 frames per second. Further details on this device can be found in Salomir et al (10).

In-house written software enabled treatment planning and on-line correction of the focal point position during the treatment to follow organ motion and avoid collateral damage of the surrounding healthy tissue, using a special TCP/IP socket which was independent of the socket dedicated to the transfer of reconstructed MR data to the external PC. The reconstructed magnitude and phase images were transferred by the standard Siemens mechanism, provided with its "Thermo" work-in-progress (WIP) package. A single Ethernet cable physically connected the local network of the MR system to the external PC (i.e., the two sockets used different ports). Original image calculation environment (ICE) program, used for the image reconstruction, was modified to facilitate the communication of MR navigator data between the MR system and a client application running on the external computer by means of the special TCP/IP socket. As soon the navigator data were available on the MR image calculation computer, the ICE program tried connecting to the external computer, and when that connection was established the navigator data was sent though. The navigator information was transferred to the external PC as absolute coordinates and the relative displacement was further calculated in the external PC application relative to the time point when the sonication started. The client application interpreted the navigator information from the MR and updated on-the-fly the RF delays of the HIFU beam-former to change the focal point position accordingly.

Description of the Experiments

A dedicated experimental set-up was designed for ex vivo measurements (see Fig. 2). The equipment was placed on the MR bed with the main axis of simulated organ motion along the direction of the main magnetic field or along the z-axis. Ex vivo tissue was placed in water coupled bath, while the inflating balloon simulated a breathing-like motion pattern, mimicking diaphragm displacement. The balloon was filled and drained by a mechanical ventilator (Anesthesia Delivery Unit (ADU^{TM}) Plus Carestation® GE Healthcare, Madison, WI). Sheep liver and a piece of turkey pectoral muscle were alternately used in the experiments. Remote control of the organ motion amplitude and period was possible from the outside the scanner room. The typical period was set in the range of 6 to 10 s.

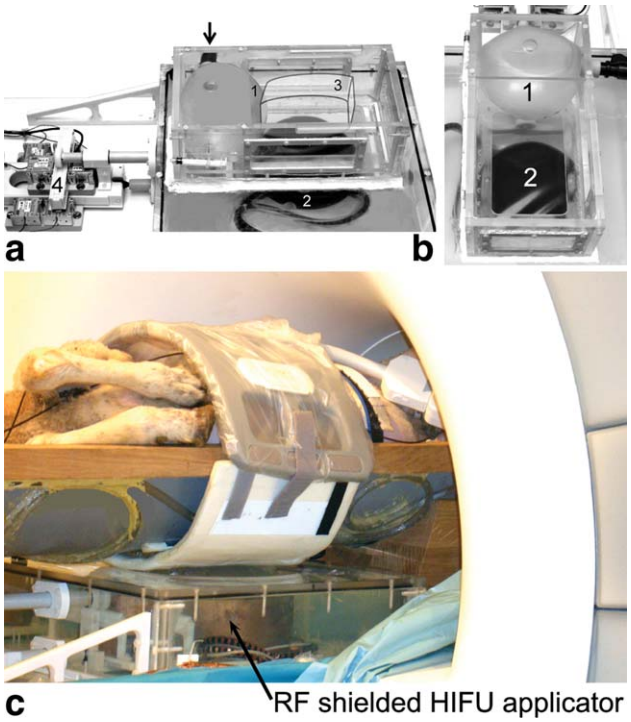

FIG. 2. **a,b:** Ex vivo experimental set-up: 1. Inflating balloon simulating breathing motion with diaphragm-like shape, 2. Water coupled bath, in which an ex vivo organ was placed, 3. Phantom, 4. Electrical motor used for positioning HIFU platform in two axis. **c:** In vivo set-up. Note the HIFU applicator and the MR coil combination.

The simulated tissue motion pattern was nonrigid with compressional deformation similar to that found in natural breathing. The nonrigid spatio-temporal rearrangement of the susceptibility distribution during motion-caused magnetic field perturbation, requiring the reference-less PRF shift thermometry to filter out this effect.

The performance of the new motion tracking method was compared in this study with "ground truth" approach, namely, the well known respiratory gated sonication and MR thermometry. This comparison took advantage of the periodic motion patterns generated by the mechanical ventilator. A "start" trigger was sent to the MR system and to the HIFU beam former when the applied air over-pressure fell below 15% of the peak value, while a "stop" trigger was sent to the HIFU beam former when the over-pressure rose above 25% of the peak value.

A standard Siemens single loop receiver coil (11 cm diameter) was used for MR signal acquisition for ex vivo experiments, while for in vivo experiments, two phased-array coils wrapped around the animal were combined (see Fig. 2c). A standard four-channel flex large coil (Siemens Medical Solutions, Erlangen, Germany) was placed on top of the abdomen, and a dedicated interventional three-channel coil (Clinical MR Solutions, Brookfield, WI, USA) with 14 × 16 cm^2 aperture, enabling HIFU beam propagation, was placed under the animal. The scanner built-in adaptive coil combine algorithm was used. The pencil-beam navigator tracked the diaphragm motion in the close proximity of the MRT slice.

Independent single-point sonications of the sheep liver in vivo were performed intercostally in two animals (both female, mean weight = 25-35 kg). Ethical approval was granted by the Geneva University Institutional Animal Care and Use Committee and by the Cantonal Veterinary Authority of Geneva. The animals were intubated and mechanically ventilated. Anesthesia was maintained by continuous inhalation of 2% isoflurane (Abbott AG, Baar, Switzerland). The breathing rate was approximately 7-10 breaths/min. The pencil beam navigator was placed parallel to the SI direction, crossing the right half of the diaphragm and avoiding the proximity of large blood vessels. A preliminary acquisition was performed to calibrate the tracking factor between the navigator measurements and the subsequent applied slice displacements. A tracking factor was considered appropriate if the anatomic structures around the planned position of the HIFU focus (mainly the blood vessels within the liver parenchyma) appeared as static in the motion-compensated GRE-EPI magnitude data. Typically, a range of tracking factors between 0.5 and 1 was tested with an incremental step of 0.05. Therefore, a maximum of 10 scout acquisitions were performed, requiring in total approximately 10 min. For the in vivo experiments, the navigator tracked organ motion over the right hemidiaphragm, which caused that the targets more distal to that tracking position required varying correction factors. A rib protection method, described in (10), was used to protect against collateral thermal damage. The animals were awoken after the experiment and followed up for 7 days. Further details on the MRgHIFU protocol in the sheep liver in vivo can be found in Auboiroux et al (19).

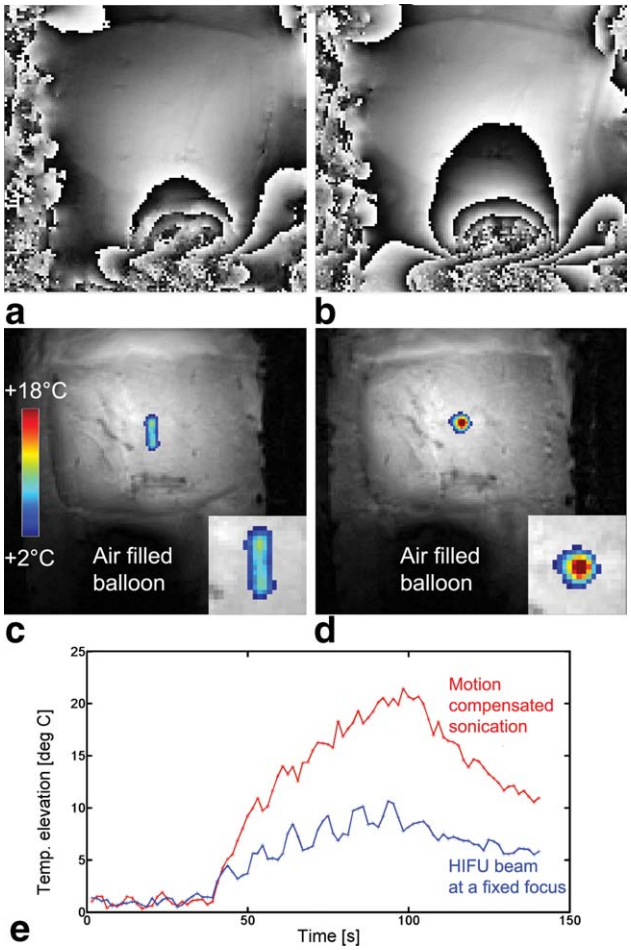

FIG. 3. Baseline phase maps of motion-compensated MR thermometry, showing significant difference in the local magnetic field due to breathing motion. Phase maps are shown at the end of (**a**) inspiration (**b**) expiration. **c,d:** Ex vivo exemplary slice tracking thermometry images showing significant difference in the thermal build-up when the HIFU focal point position was motion-compensated or not. Sonication end point thermal maps are shown: without focal point position correction (c) and with correction (d) (FOV = 192 mm). **e:** Comparison of temporal curves of temperature elevation in the highest temperature voxel corresponding to the cases (c-d), respectively.

RESULTS

Ex Vivo Experiments

On Figure 3, the need for a reference-less reconstruction method and the effectiveness of the HIFU focal point position correction for the ex vivo experiment is demonstrated. The amplitude of ex vivo muscle motion was 12 mm, while the period was 7.5 s. Every shown case on Figure 3 was acquired with slice tracking of MR thermometry. The average SNR was approximately 35. The reference-less MR thermometry method delivered a baseline stability of 0.4 ± 0.1°C.

Although the images were acquired with the motion-compensated segmented GRE-EPI sequence, inhomogeneous magnetic susceptibility field variations due to motion yielded large phase changes inside the breathing cycle (see Figs. 3a and 3b). This effect required the use of a motion-insensitive PRF shift thermometry method. The reference-less approach was chosen because of the advantageous workflow (no need to map the space of events before the treatment) and for future compatibility with free-breathing condition on patients. Repositioning of the Dirichlet's domain was not required with motion-compensated magnitude data as the tissue motion appeared motion-less.

Figure 3c corresponds to continuous HIFU sonication with a fixed focus position in a piece of moving ex vivo turkey pectoral muscle (non–motion-compensated sonication and motion-compensated MR thermometry acquisition), while for Figure 3d the focal point position was steered in real time to lock on tissue motion. It can be observed from the figure that the in-plane thermal build-up in the left image is elongated, while the one on the

right is sharply focused in one spot. The in-plane extension of the thermal build-up in the left image is around 12 mm, which corresponds well with the pre-set amplitude of motion. The maximum temperature achieved with the HIFU sonication (36 s, 108 ac W) was around 20°C in the focal spot for the compensated approach, while only around 10°C for the noncompensated. This corresponds to a ratio of 2 between the highest temperature elevations in tissue at equal HIFU energy for the compensated versus non compensated approach.

The comparative experiments conducted under various conditions: motion-compensated (new method) or non-compensated sonication in moving tissue (monitored with motion-compensated MR thermometry), respiratory gated sonication and MR thermometry (i.e., "ground truth" motion compensation) and, respectively, fixed focus sonication in static tissue (i.e. reference experiment) led to following observations based on four repeated experiments per method, see Figure 4 for exemplary results on ex vivo liver: (i) fixed focus sonication in moving tissue yielded an elongated thermal build-up, approximating the histogram of mass-point positions during the motion cycle. Motion amplitude higher than 10 mm tended to split the lesion into two separate "satellites" corresponding to the inhalation and exhalation positions; (ii) the new method of motion tracking as well as the respiratory gating sonication yielded basically isotropic thermal build-up but the ablation efficiency was significantly higher for the active motion tracking, when the duty cycle was near 100%; (iii) the reference sonication in static conditions confirmed the precise beam forming without inherent acoustic aberration. Note, a quantitative correlation ex vivo between cumulated thermal dose (31) (calculated here for a virtual baseline temperature of 37°C) and thermally decolored tissue is not meaningful as the two processes rely on different mechanisms. When considering the thermal patterns induced by the non-compensated sonication on Figure 3b (turkey pectoral muscle) and Figure 4b (sheep liver), differences could be observed, especially accentuated splitting hot spots in the second case, although the motion amplitude was comparable (12 mm and 14 mm, respectively). The different elasticity of various tissues probably yields slightly different patterns of motion during the breathing cycle, thus different histograms of mass-point position in the fixed focus reference frame and therefore different topology of the heating patterns.

In Vivo Experiments

Both sheep studies yielded similar results. On Figure 5, two images from one in vivo sheep liver sonication (40 s, 240 ac W) experiment are shown, acquired at the end of (a) inspiration and (b) expiration. The apparent motion of the ribs can be observed, although they were static, due to the use of PMC. The maximum temperature elevation was found to slightly exceed 10°C. It reached a steady state regime after approximately 30 s and longer treatment duration did not increase the temperature. The HIFU acoustic energy was delivered as a single spot. MRI follow up and animal necropsy indicated no burning of the tissue surrounding the ribs or at other abdominal interfaces for the actual conditions of sonication (power, duration, F-number and dynamic steering range). SNR of the liver MR thermometry images ranged between 20 and 25. At the given TE and B_0, this corresponds to approximately 0.5°C intrinsic standard deviation of MR thermometry (32). This is considered sufficient to enable accurate monitoring of the HIFU sonication. The combination of a limited acoustic window of intercostal sonication with conservative ribs' protection, liver perfusion and limited available acoustic power yielded insufficient temperature elevation to cause irreversible tissue damage.

DISCUSSION

Two fundamental issues of MRgHIFU treatment have been addressed in the presented work, namely the real-time control of acoustic energy targeting and motion correction of MR thermometry. The MR thermometry developments are not restricted to MRgHIFU, but are applicable to any other thermal therapy in abdomen (e.g., LITT or RFA).

Here, the monitoring of HIFU ablation was performed by PRF shift-based MR thermometry implemented by segmented GRE EPI pulse sequence. Segmented k-space acquisition was used in the phase-encode direction to minimize T_2* apodization effects on the image. The position of the focal point as well as the position of imaging slice were updated according to the organ displacement measured by the segment-based MR navigator, and thus achieving intra- and interscan MR motion compensation. The treatment described here does not rely on reconstructed magnitude nor phase MR images, and therefore potential latency from data reconstruction and export to the external computer is not involved in the feedback process. The temporal resolution of the motion correction was 80 ms, while the readout bandwidth per pixel was reduced by a factor larger than 2 as compared to the one suggested in (15). Obtained SNR was larger than 20 in vivo for a voxel volume of 0.017 mL. Because the motion compensation was applied, the imaged object appeared motion-less in the image. This allowed easier implementation of reference-less thermometry, as it was not necessary to reposition the ROI due to motion.

As the pencil-beam navigator remains the most robust organ-motion tracking method currently available on clinical MR systems, it was used for slice tracking of MR thermometry to provide accurate compensation of tissue displacement along the SI direction (i.e., principal component of motion). The correction factor of motion between the tracked diaphragm position and the ROI for sonication in liver was manually adjusted on an individual basis, aiming to cancel the apparent motion in magnitude GRE-EPI data around the location of the HIFU focus. While this empirical methodology enabled the proof of concept in vivo, the adjustment of the correction factor may be done automatically, e.g., a closed loop algorithm iteratively changing the tracking factor until nulling the motion field vectors in the MR thermometry magnitude image.

By the means of the pencil-beam navigator, the focal point position could be updated at an effective frame

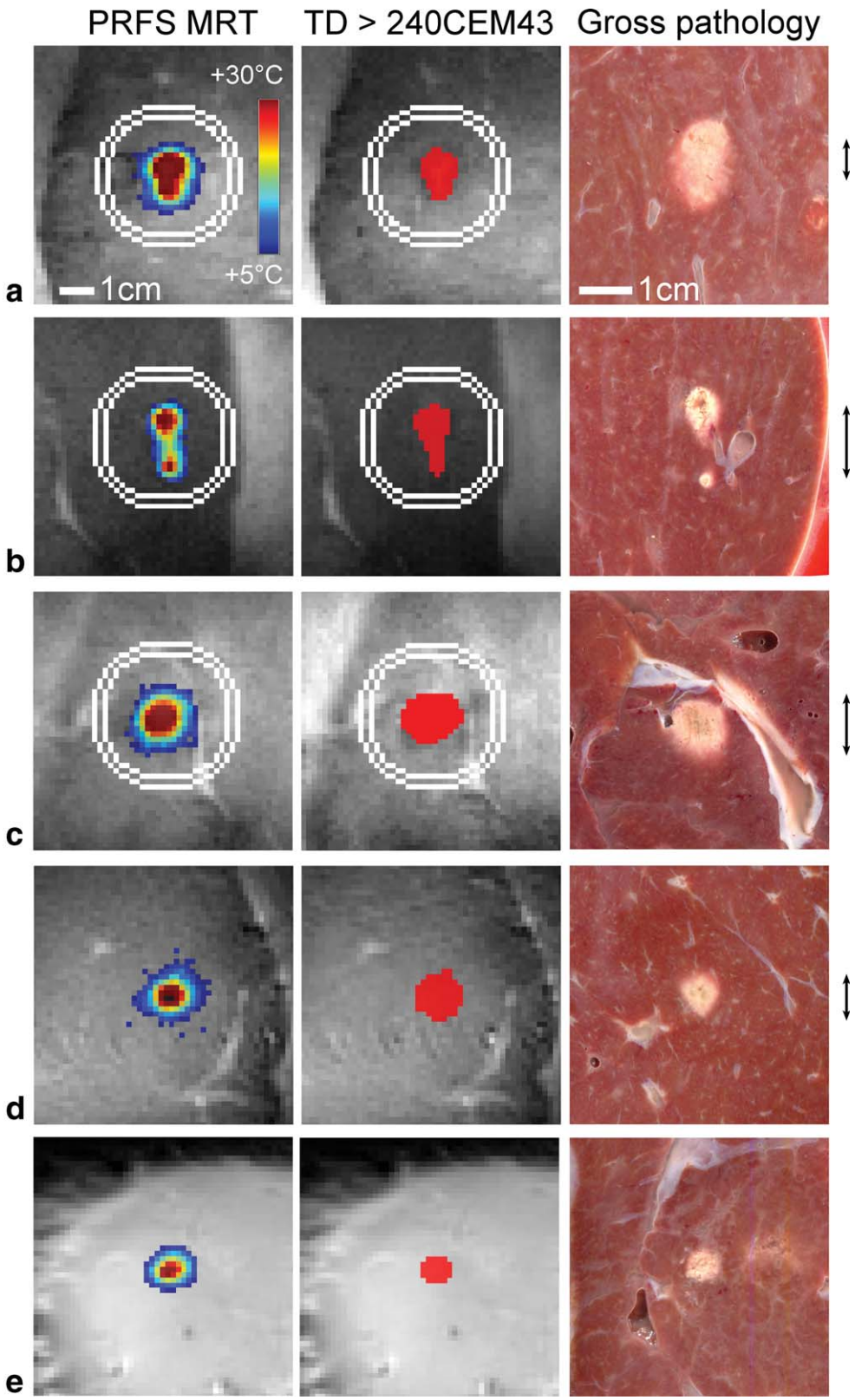

FIG. 4. Pictorial comparison between ex vivo results of MRgHIFU sonication in moving tissue. The focal plane is shown each time. Left column: MR thermometry (relative values above the baseline, see color bar) at the end-point of sonication. Middle column: cumulated thermal dose exceeding the 240CEM43 threshold. Right column: gross pathology and the amplitude of motion (double head arrow). A distance scale is provided for each type of image. When the reference-less PRF shift calculation was used for MR thermometry, the double border of the Dirichlet's domain is indicated. The sonication parameters are provided in each case as (power [W], duration [s], duty cycle [%], motion amplitude [mm]). The following conditions apply: **a:** Fixed focus sonication in moving tissue (192 W, 30 s, 100%, 8 mm). **b:** Fixed focus sonication in moving tissue with larger displacement amplitude (192 W, 30 s, 100%, 14 mm). **c:** Motion-compensated sonication using the new method of tracking (192 W, 30 s, 100%, 14 mm). **d:** Respiratory gated sonication synchronized to the quiet phase of exhalation (240 W, 60 s, 33%, 9 mm). **e:** Static sample, fixed focus sonication, i.e., reference experiment (108 W, 40 s, 100%, 0 mm). In the last case, the applied energy was deliberately lower to avoid nonlinear disruption (cavitation, boiling). Note the essentially isotropic spot of decoloration within the tissue for the three last rows.

rate of 1/TR, here 12.5 Hz. Steering the beam induced a decrease in focal point intensity, here −3 dB at 15 mm lateral steering. This condition was due to the relatively narrow radiation diagram of each elementary source of the phased-array (circular piston with the ratio diameter/wavelength = 4.2). This effect lowered the effectively delivered average energy, especially for large motion amplitudes. Upon the hardware capability, the instantaneous power may be increased as a function of beam steering to compensate for the mentioned effect.

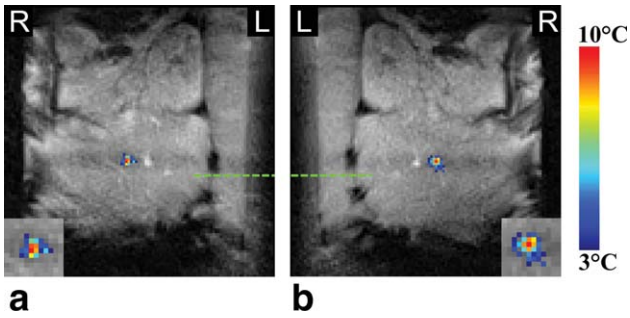

FIG. 5. In vivo exemplary thermometry images of sheep liver during motion-compensated intercostal HIFU ablation. Apparent motion of the ribs of approximately 6 mm amplitude can be observed due to the use of PMC, although the ribs were static in the laboratory frame. The thermometry images were acquired within the same breathing cycle at the end of (**a**) inspiration and (**b**) expiration (FOV = 240 mm). Note frame (a) was deliberately flipped L/R to facilitate the visual comparison of apparent motion of static structures (e.g., ribs).

In vivo experiments have demonstrated the ability of MRgHIFU treatment of moving organs, with high spatial accuracy and a near 100% duty cycle. Neither predictive modeling of organ motion nor the requirement of mapping a motion atlas before the active phase of the treatment was required. The value of the correction factor between focus and diaphragm motion was set to 0.7. The challenge of ablation through the rib cage was addressed by the use of protective reflective strips. Given the liver's anatomy of the treated animals, the focal point was positioned typically 2.5 to 3 cm behind the rib cage, yielding a significant angular masking effect of the acoustic window. By scaling the temperature elevation obtained in our experiments versus the applied power, we estimate at least twice higher acoustic output would have been necessary for effective tissue ablation in our study.

Previous studies on MRgHIFU treatment of abdominal organs (13–17) relied on heavily T_2* -weighted MR images acquired with gradient-recalled echo (GRE) single-shot echo-planar imaging (ssEPI) sequence dedicated to MR thermometry, which is generally of low contrast and limited SNR, and thus sub-optimal for motion information extraction. Because MR thermometry data, besides aiming to provide temperature maps, were also used to track organ motion, the requirement of high temporal resolution inflicted imaging with low SNR and high geometric distortion. The compulsory pretreatment data acquisition before thermal treatment renders the methods inapplicable to aperiodic free-breathing motion patterns with deep inspiration or expiration phases.

The ballistic accuracy of the MRgHIFU treatment performed in this work was not assessed. The anisotropy factor of the motion-compensated thermal build-up was found to be close to 1, and the shape of the decolorized coagulated tissue specimen in the post-operatory gross pathology ex vivo was found to be basically circular. However, positing of the focal point on a true target was not examined here. Moreover, the delivered energy was insufficient to induce in vivo thermal lesions in liver parenchyma. Although only 2 in vivo animal sonications were performed and evaluated here, our preliminary results show interesting potential of our robust treatment method, which could motivate further large scale studies to prepare clinical translation of the method.

The PRF shift reference-less approach is suitable in the presence of a large volume of unheated homogeneous tissue (e.g., liver), which provides spatial reference information. Its applicability may be challenging in a more complicated anatomic environment where susceptibility variation, adipose tissue or flow phenomena are present, e.g., prostate, breast, kidney. An extension to reference-less thermometry allowing background phase estimation in the presence of phase discontinuities between aqueous and fatty tissues was described in Rieke et al (24). That method was based on a multi-echo sequence and binary water and fat maps generated using a Dixon reconstruction.

Another limitation of the implemented method was the lack of automatic feedback control of the temperature elevation, i.e., no objective function was defined for the time course of the focal point heating. The engineering architecture of our solution is readily compatible with integration of a spatial–temporal temperature controller that will be addressed in future studies.

Only the SI component of the motion was corrected for in this study. Although this is, in general, the main component of the abdominal motion, correcting for the complete 3D motion may be required in some specific situations where the spatial accuracy is critical.

CONCLUSIONS

This study demonstrates motion compensation during MRgHIFU using prospective motion corrected segmented EPI for thermal mapping and control of the HIFU focal spot. Accurate focal point lock-on target was achieved in ex vivo moving phantoms and sheep. The proposed MR thermometry motion compensation method produced accurate temperature maps with good SNR and low geometric distortion.

ACKNOWLEDGMENTS

The authors thank Nicolin Hainc for reading and improving the manuscript. The Center of Biomedical Imaging (CIBM) – Switzerland is acknowledged for access to the MR imaging infrastructure. The authors also thank Prof. Denis Morel, Mrs. Sylvie Roulet, and Mr. Jean-Pierre Giliberto (University Medical Center, Geneva, Switzerland) for assistance with the in vivo experiments.

REFERENCES

1. Cline HE, Schenck JF, Hynynen K, Watkins RD, Souza SP, Jolesz FA. MR-guided focused ultrasound surgery. J Comput Assist Tomogr 1992;16:956–965.
2. Hynynen K, Freund WR, Cline HE, Chung AH, Watkins RD, Vetro JP, Jolesz FA. A clinical, noninvasive, MR imaging-monitored ultrasound surgery method. Radiographics 1996;16:185–195.
3. Smart OC, Hindley JT, Regan L, Gedroyc WM. Magnetic resonance guided focused ultrasound surgery of uterine fibroids – the tissue effects of GnRH agonist pre-treatment. Eur J Radiol 2006;59:163–167.
4. Tempany CM. From the RSNA refresher courses: image-guided thermal therapy of uterine fibroids. Radiographics 2007;27:1819–1826.
5. Schmitz AC, van den Bosch MA, Rieke V, Dirbas FM, Butts Pauly K, Mali WP, Daniel BL. 3.0-T MR-guided focused ultrasound for preoperative localization of nonpalpable breast lesions: an initial experimental ex vivo study. J Magn Reson Imaging 2009;30:884–889.

6. Chopra R, Colquhoun A, Burtnyk M, et al. MR imaging-controlled transurethral ultrasound therapy for conformal treatment of prostate tissue: initial feasibility in humans. Radiology 2012;265:303–313.
7. Staruch R, Chopra R, Hynynen K. Localised drug release using MRI-controlled focused ultrasound hyperthermia. Int J Hyperthermia 2011;27:156–171.
8. Civale J, Clarke R, Rivens I, ter Haar G. The use of a segmented transducer for rib sparing in HIFU treatments. Ultrasound Med Biol 2006; 32:1753–1761.
9. Quesson B, Merle M, Kohler MO, Mougenot C, Roujol S, de Senneville BD, Moonen CT. A method for MRI guidance of intercostal high intensity focused ultrasound ablation in the liver. Med Phys 2010;37:2533–2540.
10. Salomir R, Petrusca L, Auboiroux V, et al. Magnetic resonance-guided shielding of prefocal acoustic obstacles in focused ultrasound therapy: application to intercostal ablation in liver. Invest Radiol 2013;48:366–380.
11. Kopelman D, Inbar Y, Hanannel A, et al. Magnetic resonance-guided focused ultrasound surgery (MRgFUS): ablation of liver tissue in a porcine model. Eur J Radiol 2006;59:157–162.
12. Okada A, Murakami T, Mikami K, Onishi H, Tanigawa N, Marukawa T, Nakamura H. A case of hepatocellular carcinoma treated by MR-guided focused ultrasound ablation with respiratory gating. Magn Reson Med Sci 2006;5:167–171.
13. de Zwart JA, Vimeux FC, Palussiere J, Salomir R, Quesson B, Delalande C, Moonen CT. On-line correction and visualization of motion during MRI-controlled hyperthermia. Magn Reson Med 2001; 45:128–137.
14. de Senneville BD, Mougenot C, Moonen CT. Real-time adaptive methods for treatment of mobile organs by MRI-controlled high-intensity focused ultrasound. Magn Reson Med 2007;57:319–330.
15. Ries M, de Senneville BD, Roujol S, Berber Y, Quesson B, Moonen C. Real-time 3D target tracking in MRI guided focused ultrasound ablations in moving tissues. Magn Reson Med 2010;64:1704–1712.
16. de Senneville BD, Ries M, Maclair G, Moonen C. MR-guided thermotherapy of abdominal organs using a robust PCA-based motion descriptor. IEEE Trans Med Imaging 2011:30;1987–1995.
17. Holbrook AB, Ghanouni P, Santos JM, Dumoulin C, Medan Y, Pauly KB. Respiration based steering for high intensity focused ultrasound liver ablation. Magn Reson Med 2014:71;797–806.
18. von Siebenthal M, Szekely G, Gamper U, Boesiger P, Lomax A, Cattin P. 4D MR imaging of respiratory organ motion and its variability. Phys Med Biol 2007;52:1547–1564.
19. Auboiroux V, Petrusca L, Viallon M, Goget T, Becker CD, Salomir R. Ultrasonography-based 2D motion-compensated HIFU sonication integrated with reference-free MR temperature monitoring: a feasibility study ex vivo. Phys Med Biol 2012;57:N159–N171.
20. Celicanin Z, Auboiroux V, Bieri O, Petrusca L, Natsuaki Y, Santini F, Viallon M, Scheffler K, Salomir R. Hybrid US-MR Guided HIFU Treatment Method with 3D Motion Compensation. In: Proceedings of the 21st Annual Meeting of ISMRM, Salt Lake City, USA, 2013. p. 233.
21. Rieke V, Butts Pauly K. MR thermometry. J Magn Reson Imaging 2008;27:376–390.
22. Rieke V, Vigen KK, Sommer G, Daniel BL, Pauly JM, Butts K. Referenceless PRF shift thermometry. Magn Reson Med 2004;51:1223–1231.
23. Salomir R, Viallon M, Kickhefel A, et al. Reference-free PRFS MR-thermometry using near-harmonic 2-D reconstruction of the background phase. IEEE Trans Med Imaging 2012;31:287–301.
24. Rieke V, Kinsey AM, Ross AB, Nau WH, Diederich CJ, Sommer G, Pauly KB. Referenceless MR thermometry for monitoring thermal ablation in the prostate. IEEE Trans Med Imaging 2007:26:813–821.
25. Davies SC, Hill AL, Holmes RB, Halliwell M, Jackson PC. Ultrasound quantitation of respiratory organ motion in the upper abdomen. Br J Radiol 1994;67:1096–1102.
26. von Siebenthal M, Szekely G, Lomax A, Cattin P. Inter-subject modeling of liver deformation during radiation therapy. Med Image Comput Comput Assist Interv 2007;10:659–666.
27. Ehman RL, Felmlee JP. Adaptive technique for high-definition MR imaging of moving structures. Radiology 1989;173:255–263.
28. McConnell MV, Khasgiwala VC, Savord BJ, Chen MH, Chuang ML, Edelman RR, Manning WJ. Prospective adaptive navigator correction for breath-hold MR coronary angiography. Magn Reson Med 1997;37:148–152.
29. Hardy CJ, Pearlman JD, Moore JR, Roemer PB, Cline HE. Rapid NMR cardiography with a half-echo M-mode method. J Comput Assist Tomogr 1991;15:868–874.
30. Nehrke K, Bornert P, Groen J, Smink J, Bock JC. On the performance and accuracy of 2D navigator pulses. Magn Reson Imaging 1999;17: 1173–1181.
31. Sapareto SA, Dewey WC. Thermal dose determination in cancer therapy. Int J Radiat Oncol Biol Phys 1984;10:787–800.
32. Salomir R, Palussiere J, Vimeux FC, de Zwart JA, Quesson B, Gauchet M, Lelonq P, Perqrale J, Grenier N, Moonen CT. Local hyperthermia with MR-guided focused ultrasound: spiral trajectory of the focal point optimized for temperature uniformity in the target region. J Magn Reson Imaging 2000:12; 571–582.